# CHAPTER VII
# IN VITRO AND IN VIVO RELEASE OF BASIC FIBROBLAST GROWTH FACTOR USING A SILK FIBROIN SCAFFOLD AS THE DELIVERY CARRIER

## 7.1 Abstract

The objective of this study was to examine the *in vitro* and *in vivo* release behavior of basic fibroblast growth factor (bFGF) by using silk fibroin as a carrier matrix. Two different solvents were used to prepare two types of silk fibroin scaffolds via the salt-leaching technique, i.e. hexafluoroisopropanol (HFIP) for HFIP-derived processing and water for aqueous-derived processing. It was found that the average pore size of HFIP-derived and aqueous-derived silk fibroin scaffolds was 479±130 and 473±146 μm, respectively. The *in vitro* release study suggests that the opposite charge between the silk fibroin and the bFGF at physiological pH rendered them to form a complex, and the difference in the mode of processing to produce the silk fibroin scaffold did not affect the affinity to bFGF. However, a higher degradation of the aqueous-derived silk fibroin scaffolds provided higher *in vitro* release kinetics of the bFGF, as compared to the HFIP-derived scaffolds. From the *in vivo* study, the use of silk fibroin scaffolds as the carrier matrix enabled the control of the *in vivo* release of bFGF in a sustainable fashion over 2 weeks, while the majority of the bFGF disappeared within one day after the injection of the bFGF in soluble form. In addition, the *in vivo* release of bFGF from the silk fibroin scaffolds was not affected by the mode of processing due to their similar short-term degradation behavior *in vivo*. This study demonstrates the promising use of different preparation processes for the production of a three-dimensional porous silk fibroin scaffold as the bFGF carrier for tissue engineering applications.

**Keyword:** silk fibroin; basic fibroblast growth factor; bFGF; delivery

## 7.2 Introduction

Basic fibroblast growth factor (bFGF) was originally characterized *in vitro* as a growth factor for fibroblasts and capillary endothelial cells, while *in vivo* bFGF was reported as a potent mitogen and chemoattractant for a wide range of cells (Tabata et al., 2005b). bFGF has also been known to stimulate the regeneration of a broad range of tissues, including cartilage, nerves, skin, liver, and blood vessels (Jeon et al., 2005). The administration of bFGF has shown therapeutic potential for tissue regeneration (Nicole et al., 1994; Ono et al., 1995; Chen et al., 1992; Radomsky et al., 1998). However, the bioactivity of bFGF cannot always be expected when it is injected in the soluble form into the body, because of its short duration of retention at wound sites and short half-life caused by susceptibility to enzymatic degradation *in vivo*. The administration of bFGF may be greatly improved by the use of controlled-delivery systems, allowing sustained and localized release, thereby enhancing the therapeutic efficacy (Tabata, 2005b). Based on advances in the tissue-engineering approach by combination with a controlled-delivery system, a carrier for growth factor delivery should consist of a three-dimensional scaffold that is able to deliver protein over the required physiological timeframe without compromising the bioactivity upon release. In addition, the scaffolds should provide physical support for cell adhesion and growth and be biodegraded at a rate commensurate with new extracellular matrix (ECM) production (Tabata et al., 2005b).

A number of polymeric carriers with or without chemical modification, including collagen (Kanematsu et al., 2004), gelatin (Tabata et al., 1994, 1999a, 1999b), chitosan (Fujita et al., 2005), hyaluronan (Pike et al., 2006), fibrin derivatives (Sakiyama-Elbert & Hubbell, 2000), and poly(lactide-co-glycolide) (PLGA) (Shen et al., 2008), are used to control the release of bFGF. Although these materials are biocompatible and provide sustainable delivery of bFGF while retaining its bioactivity, they have a common disadvantage of poor mechanical properties. Hence, several

physical modifications have been reported, such as reinforcement with a filler to enhance their mechanical properties (Lind et al., 2001; Hokogu et al., 2006); however, the complicated process and careful control are needed. Silk fibroin, derived from the silk of the silkworm *Bombyx Mori*, is a very attractive scaffolding material and has impressive mechanical properties, compared to commonly used polymers, both natural and synthetic (Kim et al., 2005b). Silk fibroin is less immunogenic and inflammatory, compared to either collagens or PLGA (Meinel et al., 2005). Even though silk fibroin may exhibit excessively slow biodegradation *in vivo*, its degradation, which is related to the mode of processing, can certainly be improved (Jin et al., 2005; Kim et al., 2005b).

There are three techniques that have been widely used to produce the three-dimensional porous scaffolds for silk fibroin, i.e. electrospinning, freeze-drying, and salt leaching. Among them, the salt-leaching technique has received more attention in recent years (Meinel et al., 2004a, 2004b, 2006; Kim et al., 2007; Wang et al., 2005, 2006), because this technique produces a silk fibroin scaffold having high porosity, an interconnected pore network, and a controllable pore size (Kim et al., 2005a, 2005b). Despite the fact that the salt-leached silk fibroin scaffolds have been shown to be suitable substrates of human mesenchymal stem cells (hMSCs) for the *in vitro* engineering of bone-like (Meinel et al., 2004b, 2006; Kim et al., 2007) and cartilage-like tissue (Meinel et al., 2004a; Wang et al., 2005, 2006) under appropriate culture conditions without incorporating growth factor into the matrix, the incorporation of bFGF into the silk fibroin scaffold may reduce the culture/regeneration time and improve the quality of successful tissue repair in either *in vitro* culture of cellular constructs or the *in vivo* repair of defects.

The preparation of a silk fibroin scaffold via the conventional salt-leaching technique required the use of organic solvent for both the dissolution of silk fibroin and treatments of the regenerated-solidified materials to control structure and stability of the scaffold in aqueous environments, while the unconventional salt leaching, which was first proposed by Kim et al. (2005b), is an all-aqueous-based system throughout the preparation process. Interestingly, it was demonstrated that the aqueous-derived silk

fibroin scaffolds showed higher *in vitro* and *in vivo* degradation than the organic-derived scaffolds (Kim et al., 2005b; Wang et al., 2008). Therefore, the use of different modes of processing to fabricate the silk fibroin scaffold may benefit the tailoring of the protein delivery where release kinetics depends on the carrier's degradation (erosion-controlled release).

This present study was designed to prepare silk fibroin scaffolds by either organic-derived or aqueous-derived processing. The organic solvent used for organic-derived processing was hexafluoroisopropanol (HFIP). The study was focused on the delivery behavior of bFGF — whether or not the silk fibroin scaffold is able to sustain the release of bFGF, as well as whether or not the degradation, adjusted by using different preparation processes, affects the release kinetics of bFGF. The release of bFGF from HFIP-derived or aqueous-derived scaffolds was compared both *in vitro* and *in vivo*. The affinity between silk fibroin and bFGF is discussed. Additionally, the *in vitro* and *in vivo* degradation of the silk fibroin scaffolds prepared by different modes of processing was compared. The relationship between biodegradation and chain entanglement is also discussed.

## 7.3 Experimental

### 7.3.1 Materials

Raw silk fibers of *Bombyx Mori* were obtained from the Queen Sirikit Sericulture Center, Saraburi Province, Thailand. Radioisotope $Na^{125}I$ (740 MBq/mL in 0.1 N NaOH aqueous solution) and N-succinimidyl-3-(4-hydroxy-3-di[$^{125}$I]iodophenyl) propionate, or $^{125}$I-Bolton-Hunter Reagent (NEX-120H), (147 MBq/ml in anhydrous benzene) were supplied by NEN Research Products (DuPont, Wilmington, Del., USA). Human recombinant bFGF, with an isoelectric point of 9.6, was purchased from Kaken Pharmaceutical Co., Tokyo, Japan. All other chemicals were reagent grade and were used as received.

7.3.2 Preparation of regenerated silk fibroin solution

The preparation of the fibroin solutions was previously described (Wongpanit et al., 2007). Briefly, the raw silk fibers of *Bombyx mori* were boiled for 15 min in an aqueous solution of 0.5% $Na_2CO_3$ and were then rinsed thoroughly with water. This process was repeated. After drying at 40°C, the degummed silks were dissolved in $CaCl_2$:Ethanol:$H_2O$ (molar ratio = 1:2:8) at 78°C and the silk dissolution was completed within 15 min. The solution was subsequently dialyzed against double-distilled water (DDW) for 4 days (changing the media twice a day), followed by centrifugation at 10,000 rpm for 10 min. The centrifugation was repeated twice. The as-prepared regenerated silk fibroin concentration was 6.32 wt%. The silk fibroin solution was then heated up ~ 60°C under slow stirring to evaporate the water to reach the final concentration of 12 wt% (Chen et al., 2006).

7.3.3 Preparation of the silk fibroin scaffolds

The HFIP-derived silk fibroin scaffolds were prepared from a freeze-dried silk fibroin that was re-dissolved in HFIP to obtain a 9 wt% solution. The scaffolds were prepared in a disk-shaped perfluoroalkoxy (PFA) container with a 1.8 cm diameter by adding 1.8 grams of granular NaCl particles (500–600 μm) into 0.6 ml of 9 wt% silk fibroin in HFIP. The container was covered and left overnight at 4°C for homogeneous salt distribution. The solvent was then evaporated at room temperature for 3 days. The silk/porogen matrix was treated in a 90% (v/v) methanol solution for 30 min to induce the formation of the β-sheet structure. The matrices were immersed in DDW for 2 days to remove the salts, and were subsequently air-dried. The aqueous-derived silk fibroin scaffolds were prepared by adding 2.1 grams of granular NaCl particles (500–600 μm) into 0.9 ml of 12 wt% aqueous silk fibroin solution in a PFA container. The containers were covered and left at 30°C for 24 hours, followed by immersion for 2 days in DDW to extract the salt (Kim et al., 2005b).

The obtained silk fibroin scaffolds from both HFIP-derived and aqueous-derived processing were shaped into smaller pieces 4 mm high and 5 mm in diameter

using a metallic-hole puncher. The average pore size of the HFIP-derived and aqueous-derived silk fibroin scaffolds was 479±130 and 473±146 μm, respectively.

7.3.4 Morphology of the silk fibroin scaffolds

To observe the cross-section of the scaffold, both HFIP-derived and aqueous-derived silk fibroin scaffolds were carefully cut with a razor blade. The cross-sections of the scaffolds were coated with platinum on the ion sputter (E- 1010, Hitachi, Tokyo, Japan) at 50 mTorr and 5mA for 3 min. The inner microstructure of the scaffolds was observed by a scanning electron microscope (SEM) (S-2380N, Hitachi, Tokyo, Japan) at a voltage of 10 kV.

7.3.5 *In vitro* enzymatic degradation

The degradation of the silk fibroin scaffolds was evaluated using protease type XIV from *Streptomyces griseus* (EC 3.4.24.31, Sigma-Aldrich) as an enzyme. The scaffolds were incubated in 1 ml of phosphate-buffer saline pH 7.4 (PBS) containing the protease at 37°C under strong shaking. The enzyme concentrations used in this test was 0.05 or 0.5 $mg \cdot ml^{-1}$. The enzyme solution was replaced with freshly prepared solution daily. The scaffolds submerged in PBS without enzyme served as a control. After reaching the desired time, the scaffolds were washed twice with DDW, followed by air-drying at 30°C overnight. The dried scaffolds were kept in desiccators at least one day prior to weighing.

7.3.6 Radiolabeling of silk fibroin scaffolds

The silk fibroin scaffolds were radiolabeled according to the method of Tabata et al. (1999b). Briefly, 100 μl of $^{125}I$ Bolton–Hunter reagent solution in anhydrous benzene was bubbled with dry nitrogen gas until the benzene evaporation was complete. Then, 125 μl of 0.1 M sodium borate-buffered solution (pH 8.5) was added to the dried reagent, followed by pipetting to prepare an aqueous $^{125}I$ Bolton–Hunter solution. The silk fibroin scaffolds were impregnated with the prepared aqueous solution

at a volume of 25 μl per scaffold overnight. The radio-labeled scaffolds were then rinsed with DDW by exchanging it periodically at 4°C for 7 days to exclude non-coupled, free $^{125}$I-labeled reagent from $^{125}$I-labeled silk fibroin scaffolds.

7.3.7 Radioiodination of bFGF

The bFGF was radioiodinated according to a chloramine T method (Greenwood et al., 1963). Aqueous solution of bFGF at 0.5 mg/ml (450 μl) was added to 100 μl of a 0.5 M potassium-phosphate buffered (KPB) solution (pH 7.5). Then, 5 μl of Na$^{125}$I solution and 100 μl of 0.05 M KPB solution (pH 7.2) containing 0.06 mg of chloramine T were added to the bFGF solution. After agitation at room temperature for 2 min, 100 μl of 0.01 M PBS containing 0.12 mg of sodium metabisulfate was added to stop the radioiodination. The mixture was passed through a column of Dowex resin to remove uncoupled, free $^{125}$I molecules, followed by the addition of 650 μl of water to obtain an aqueous solution of $^{125}$I-labeled bFGF.

7.3.8 *In vitro* bFGF release

In order to incorporate $^{125}$I-labeled bFGF into both the HFIP-derived and the aqueous-derived silk fibroin scaffolds, 20 μl of the $^{125}$I-labeled bFGF solution was dropped onto the scaffolds. The absorption process was allowed to occur at 4°C overnight. The obtained $^{125}$I-labeled bFGF-impregnated silk fibroin scaffolds were then used for *in vitro* and *in vivo* bFGF release studies.

The *in vitro* release of $^{125}$I-labeled bFGF from the $^{125}$I-labeled bFGF-impregnated silk fibroin scaffolds was first conducted in PBS. After periodic replacement with PBS for 24 hours, the release behavior of the bFGF in enzyme solution was then investigated. Briefly, $^{125}$I-labeled bFGF-impregnated silk fibroin scaffolds were placed into 1 ml of the PBS. The PBS was periodically replaced at 0.5, 1, 2, 4, 8, and 12 hours. At 24 hours, the release media, neat PBS, started to be replaced by PBS containing protease at 0.05 or 0.5 mg·ml$^{-1}$ in order to observe the influence of the enzymatic degradation of the scaffolds on the release of the bFGF. The enzyme solution

was daily replaced with a freshly prepared solution. The release of bFGF was calculated by measuring the radioactivity of the release solution divided by the total radioactivity of the $^{125}$I-labeled bFGF in the scaffolds using a gamma counter (ARC-301B, Aloka, Tokyo, Japan). The total radioactivity of the $^{125}$I-labeled bFGF in the scaffolds was obtained by the sum of the radioactivity remaining in the scaffolds plus the cumulative radioactivity of the bFGF released. The natural decay of the radionuclide was adjusted using a control solution of the $^{125}$I species.

7.3.9 Estimation of *in vivo* bFGF release

To evaluate the *in vivo* release of bFGF from the silk fibroin scaffolds, the $^{125}$I-labeled bFGF-impregnated silk fibroin scaffolds were subcutaneously implanted into a pocket created in the backs of 4-week-old female ddY mice under pentobarbital anesthesia (Tabata et al., 1999b). As a control, 100 μl of an aqueous solution of the $^{125}$I-labeled bFGF was subcutaneously injected into the backs of the mice. The mice were sacrificed at 1, 3, 7, 14, 20, and 26 days. The radioactivity remaining in the scaffolds and local tissue were measured using a gamma counter (n=3 for each time point). The remaining radioactivity percentage was calculated by dividing the radioactivity remaining in the scaffold by its initial radioactivity.

7.3.10 Estimation of *in vivo* degradation of silk fibroin scaffolds

The *in vivo* degradation of the scaffolds was evaluated in terms of the radioactivity remaining in the $^{125}$I-labeled silk fibroin scaffolds after implantation in the backs of mice (Tabata et al. 1999b). At different time intervals, the mice were sacrificed and the radioactivity remaining in the scaffolds and local tissue was measured using a gamma counter (n=3 for each time point). The percentage of radioactivity remaining was calculated by dividing the radioactivity remaining in the scaffold by its initial radioactivity.

## 7.4 Results and Discussion

7.4.1 Morphology of silk fibroin scaffolds

As stated, silk fibroin is very attractive as a scaffolding material. The utility of silk fibroin as tissue-engineering scaffolds has been emphasized—for the regeneration of cartilages (Meinel et al., 2004a ), bones (Meinel et al., 2004b & 2006; Karageorgiou et al., 2006; Marolt et al., 2006; Hofmann et al., 2007), nerves (Uebersax et al., 2007), annulus fibrosus (Chang et al., 2007), or ligaments (in the form of native fibers) (Liu et al., 2007, 2008)—because these tissue structures require stability and strength, which may benefit from longer-lasting material like silk fibroin (Levenberg & Langer, 2004). A number of works have attempted to extend the biomaterial utility of silk fibroin by blending with another degradable polymer (Wongpanit et al., 2007b), reducing the β-sheet content (Jin et al., 2005), or using the aqueous-derived salt-leaching technique (Kim et al., 2005b), in order to improve its degradability.

As mentioned above, the silk fibroin scaffolds derived from the salt-leaching technique have been shown to support the proliferation and differentiation of hMSCs (Meinel et al., 2004a, 2004b, 2006; Wang et al., 2005, 2006; Kim et al., 2007). It is known that there are three key factors comprising body tissue: 1) cells, 2) the ECM for cell proliferation and differentiation, and 3) growth factors (Tabata, 2005b). Thus, in addition to the ability to provide the support of the proliferation and differentiation of the cells, the scaffold should provide the appropriate micro-environment to facilitate tissue regeneration by taking the therapeutic potential of the growth factor. However, the release of the growth factor must first be studied; whether or not silk fibroin is able to deliver the desired growth factor and which factors govern its release characteristic.

Prior to addressing the objectives of this research, the morphology of the silk fibroin scaffolds prepared by different modes of processing should be characterized. Figure 7.1 shows the SEM micrographs of both the HFIP-derived and the aqueous-derived silk fibroin scaffolds. It was observed that the pore size of the HFIP-derived (479±130 μm) and the aqueous-derived (473±146 μm) silk fibroin scaffolds were comparable. As shown in Figure 7.1, the HFIP-derived scaffold had a relatively thin

wall in the pore structure, while the aqueous-derived scaffold had thicker walls with many micro-voids inside. The formation of micro-void inside the scaffold's wall may occur from the dissolution of the imperfect self-assembly of the silk fibroin chains during the preparation step.

### 7.4.2 *In vitro* study

In this section, the degradation of the silk fibroin scaffolds and the release of the bFGF *in vitro* were studied, and the affinity between silk fibroin and bFGF was also discussed. Figure 7.2 illustrates the *in vitro* degradation of the HFIP-derived and aqueous-derived silk fibroin scaffolds submerged in enzyme solution at a concentration of either 0.05 or 0.5 $mg \cdot ml^{-1}$, with changing the solution daily. The enzyme used in this experiment was protease type XIV because the protease was widely used to examine the degradation of silk fibroin (Jin et al., 2005; Kim et al., 2005b; Wongpanit et al., 2007b). At an enzyme concentration of 0.05 $mg \cdot ml^{-1}$ (see Figure 7.2A), the weight of the HFIP-derived scaffolds was only slightly decreased after 17 days, while that of the aqueous-derived scaffolds was gradually decreased and finally remained at only 20%. By increasing the enzyme concentration to 0.5 $mg \cdot ml^{-1}$ (see Figure 7.2B), the degradation was enhanced, i.e. the weight of the HFIP-derived scaffolds was steadily decreased and remained at almost 40% of their initial weights after 17 days. In contrast, the aqueous-derived scaffolds were fully degraded within 5 days. From the results, it can be concluded that the *in vitro* degradability of the aqueous-derived scaffolds was higher than that of the HFIP-derived scaffolds, and the degradation of the scaffolds was increased with increasing enzyme concentration. These results are similar to the work of Kim et al. (2005b) who compared the degradability of the silk fibroin scaffolds prepared from different modes of processing via the salt-leaching technique.

It is known that the β-sheet, one of the crystal structures, is strongly responsible for the slow degradation of the silk fibroin, so the reduction of the β-sheet content in the silk fibroin material can enhance its degradability (Jin et al., 2005). The difference in the β-sheet content (crystallinity) of the compared scaffolds may cause the

different degradation behavior. It is well accepted that Fourier-transform infrared (FT-IR) spectroscopy and X-ray diffraction (XRD) are very useful techniques to characterize the crystal structure of silk fibroin. However, Kim et al. (2005b) reported that the structure of the HFIP-derived and aqueous-derived scaffolds could not be distinguished by data obtained from FT-IR and XRD (Kim et al., 2005b). They also found the the crystallinity of those scaffolds had similar content, i.e. around 48% (Kim et al., 2005b). Our FT-IR data also agree with Kim et al. (2005b) (data not shown). The same results were found in the work of Wang et al. (2008), i.e. the crystallinity of the HFIP-derived and aqueous-derived scaffolds determined from XRD data was also not significantly different (between 45 and 50%). Thus, at this point, by analyzing the FT-IR and XRD results, the structure of those two types of scaffolds was not different, even though they exhibited different biodegradation behaviors. In the other words, the FT-IR and XRD technique can not be used to distinguish the very tiny difference in the scaffolds prepared by different modes of processing.

In order to further analyze the different degradation behaviors of the scaffolds by their structure, the solution properties of the silk fibroin in each solvent for preparing each scaffold must be considered. The HFIP-derived scaffolds were prepared by dissolving the silk fibroin in HFIP, while the aqueous-derived scaffolds were prepared by dissolving the silk fibroin in water. In the following paragraphs, the chain entanglements of silk fibroin in the solution, correlated to the electro-spinnability, will be briefly described. In addition, the chain entanglement will be used to propose and explain why the degradation behavior of the scaffolds prepared by different modes of processing was different.

It has been demonstrated that silk fibroin both in HFIP and in water were spinnable to form the electrospun fibers. However, the lowest spinnable concentration of silk fibroin dissolved in HFIP (0.74 wt%) (Zarkoob et al., 1998, 2004) to produce the electrospun-continuous fibers was very much lower than that of the silk fibroin in water (more than 30 wt%) (Chen et al., 2006). During the electrospinning of the polymer solution, an increase in polymer concentration results in the following morphological

progression: 1) beads only, 2) beads with incipient fibers, 3) beaded fibers, and 4) fibers only. The formation of chain entanglements has been acknowledged as the primary effect in this progression (Shenoy et al., 2005; Tao & Shivkumar, 2007). Insufficient chain entanglement results in bead formation; whereas a high number of chain entanglements allows the polymer solution to form continuous fibers. It was reported that the concentration of silk fibroin in HFIP to form the electrospun fibers was just 0.74 wt%, while that of silk fibroin in water required up to >30 wt%. In this present study, the concentration used to prepare the HFIP-derived and aqueous-derived scaffolds were quite close to each other (9 wt% and 12 wt%, respectively). Thus, the number of chain entanglements of the silk fibroin in HFIP was very much higher than in water at the preparing conditions. Although the addition of NaCl particles into the silk fibroin solution eventually induced the β-sheet formation in the case of the aqueous-derived process (Kim et al., 2005b), the salt did not disturb the chain entanglement because the salt just acted as the dehydrator and the silk fibroin chains gradually folded themselves (self-assembly) under static conditions to form an insoluble order structure.

Additional information that can be used to confirm a higher number of the chain entanglements of the HFIP-derived scaffolds is their cracking behavior. When the HFIP-derived scaffolds were compressed under dried state to become the permanent deformation, the scaffolds displayed only shape change in their thickness, while the aqueous-derived scaffolds were broken into many small pieces. This is attributable to the adjacent chains that entangled with the dislocated chain, due to the external force, kept the structural integrity. Therefore, higher chain entanglements caused better structural integrity.

However, the point is how the chain entanglement is connected to the degradation behavior of the scaffolds. Considering the enzymatic degradation process, the active site of the enzyme attacka the silk fibroin resulting in the creation of small fibroin fragments. If the material has high chain entanglement, the small fibroin fragments obtained from the enzymatic digestion would be more retarded to form the soluble compound by entangling with the adjacent fibroin chains. Thus, the chain

entanglement is most likely to be the cause of the different degradation behavior. In conclusion, the HFIP-derived scaffolds degraded slower than the aqueous-derived scaffolds due to higher chain entanglement in the material.

After the degradation of each scaffold was studied and compared, the release of bFGF from both types of scaffolds would then be investigated to determine whether the difference in the degradability of the scaffolds can affect the release of bFGF or not. There are two possible methods to incorporate bFGF into the silk fibroin scaffold, i.e. 1) mixing bFGF with the polymer solution prior to fabrication (Li et al., 2006; Uebersax et al., 2007 & 2008), or 2) incorporating the bFGF after material forming (Huang et al., 2007). In this present study, the incorporation of bFGF by the first technique was not employed because there are many steps of rinsing the scaffolds during preparation. The incorporation of bFGF into the silk fibroin scaffolds was therefore carried out by impregnating the scaffolds with 20 µl of the $^{125}$I-labeled bFGF solution overnight at 4°C. The bFGF molecules were radio-labeled due to the ease of tracking their release. Two commercial medical products for bone repair also use the impregnating technique to incorporate a bone morphogenetic protein (BMP) (Luginbuehl et al., 2004). Figure 7.3 illustrates the release profile of bFGF from HFIP-derived and aqueous-derived scaffolds incorporating bFGF by submerging the scaffolds in PBS under strong shaking at 37°C. As shown in the Figure, the bFGF immediately diffused from the scaffolds within the first 2 hours. Then, the release of bFGF from both types of scaffolds gradually reached a plateau at a release fraction of about 30% after 24 hours. Even though the release of bFGF was performed in PBS for an additional 7 days, the bFGF was not much further released from the scaffolds. It should be noted that the percentage of bFGF released from the HFIP-derived and aqueous-derived scaffolds in PBS after 8 days under strong shaking was 32.1±2.8 and 38±9.9, respectively (see Figure 7.4). This release behavior indicates that silk fibroin and bFGF have strong interaction with each other because the majority of the bFGF still remained in the scaffolds, even after extensive rinsing by PBS. In addition, the different modes of processing to produce the silk fibroin scaffolds did not affect the affinity to bFGF

because they had the similar pattern of release profile as well as the amount of bFGF released. However, it was observed that around one third of the bFGF released suddenly from the scaffolds due to the incomplete complexation process between the bFGF and the silk fibroin scaffolds after bFGF impregnation. Similar results were also observed in the case of the delivery of BMP-2 by silk fibroin scaffolds. There was an initial burst in the BMP-2 release profile from BMP-2-impregnated silk fibroin scaffolds, and the release of BMP-2 eventually reached the plateau at the release fraction of 75% after 1 week (Karageorgiou et al., 2006). It is important to note that the increase of impregnation temperature and/or duration promoted the complexation process of bFGF to the hydrogel (Tabata et al., 1998). The amount of non-complexed bFGF in our system (~30%) was much lower than that in the non-complexed BMP-2 (~75%). This is likely because of the longer duration of sorption of the bFGF (overnight) to the scaffold compared to the shorter adsorption time of the BMP-2 (6 hours).

The bFGF is also referred to as one of the heparin-binding growth factors (Mizumo et al., 1994; Tesser et al., 1994). Physiologically, the numerous growth factors bind the highly anionic, sulfated glycosaminoglycan heparin with high affinity. This binding activity is important in sequestering the growth factors in the ECM, and in serving to localize growth factor activity and prevent growth factor degradation (Roghani et al., 1994). Interactions between the growth factor and heparin occur in part by shape recognition, but primarily by electrostatic attractions between the N- and O-sulfated residues of heparin, and the lysine and arginine residues of the growth factors (Godspodarowicz et al., 1986; Wissink et al., 2000). Accordingly, heparin has been incorporated into many hydrogel delivery systems to promote the biological function by an increase in the affinity (Wissink et al., 2000; Pike et al., 2006). Thus, it is postulated that the high affinity between the silk fibroin (isoelectric point, pI 3.8-4.5, see Table 7.1) and the bFG (pI 9.6) as discussed above was based on the electrostatic interaction. In fact, the growth factor-releasing scaffold using silk fibroin as the carrier matrix based on the electrostatic interaction, has been shown to prolong the release of many growth factors under *in vitro* non-degradation conditions, including BMP-2 (pI 8.5)

(Karageorgiou et al., 2006; Li et al., 2006), nerve growth factor (pI 9.3), and insulin-like growth factor I (pI 8.3) (Uebersax et al., 2007 & 2008), and still retained their bioactivity upon release. It should be noted that in addition to the diffusion of the non-complexed growth factor at the beginning of the release, the release of the growth factor under non-degradation condition is governed by a thermodynamic equilibrium mechanism between free growth factor in the release medium and the growth factor bound to the carrier.

After the release of bFGF was studied under the non-degradation conditions for 24 hours in PBS, the release of bFGF was further continuously investigated by replacing the release media from neat PBS to PBS containing enzyme to observe the release behavior under *in vitro* enzymatic degradation conditions (see Figure 7.4). The release solution containing the enzyme was replaced daily. It was found that the initial burst release of bFGF was also observed for both types of scaffolds, regardless of enzyme concentration after the first day (see Figure 7.4). The burst release of bFGF after the addition of enzyme, along with the *in vitro* degradation study, suggests that most of the bFGF molecules, which were suddenly released from the scaffolds due to the degradation of silk fibroin, existed in a superficial layer of the scaffold's wall. This further indicates that the majority of the bFGF (around three fourths of the bFGF incorporation, see Figure 7.4) during impregnation into the silk fibroin scaffold cannot reach the deeper parts of the scaffold's wall.

Considering the bFGF release at an enzyme concentration of 0.05 $mg \cdot ml^{-1}$ (see Figure 7.4A), the initial amount of the burst release of bFGF (75.7±1.8 %) from the HFIP-derived scaffolds was statistically significantly lower than that of bFGF released (83.5±1.9%, $p<0.05$) from the aqueous-derived scaffolds. Then, the bFGF in the HFIP-derived and the aqueous-derived scaffolds gradually released and reached the release fractions of 89.0±1.6 and 96.5±1.5%, respectively at the seventh day. These results, together with the *in vitro* degradation study, suggest that a slower release of bFGF from HFIP-derived scaffolds, as compared to that from the aqueous-derived scaffolds, can be attributed to their slower degradation. As the enzyme concentration was increased to 0.5

$mg \cdot ml^{-1}$ (see Figure 7.4B), a stronger initial burst release of bFGF was observed. However, there was no statistical difference between the bFGF released from the HFIP-derived and the aqueous-derived scaffolds due to their very strong degradation.

The results of this section demonstrate that the opposite charge between silk fibroin and bFGF at physiological pH rendered them able to form a complex. The preparation of the silk fibroin scaffolds via the aqueous-derived technique enabled the improvement in the *in vitro* degradation of silk fibroin because of less chain entanglement in the material. In addition, a higher amount of degradation of the aqueous-derived scaffolds provided higher release kinetics (at a lower enzyme concentration) as compared to that of the HFIP-derived scaffolds. However, the *in vivo* degradation of both types of scaffolds as well as the *in vivo* release of bFGF needed to be further characterized because there are much more complicated processes under the *in vivo* situation in response to the implanted materials than the simple *in vitro* study.

### 7.4.3 *In vivo* study

In order to study the degradation of the silk fibroin scaffolds *in vivo*, the scaffolds need to be radio-labeled using the $^{125}I$ Bolton-Hunter reagent to track the extent of the scaffold's degradation. The $^{125}I$ Bolton-Hunter reagent reacted with the free amino groups of the protein molecules under mild conditions to attach the $^{125}I$-labeled groups by amide bonds (Bolton and Hunter, 1973). After allowing the reaction to proceed overnight, the scaffolds were extensively rinsed with water to remove the uncoupled $^{125}I$ reactants. Then, a study of the scaffold's degradation was conducted by the subcutaneous implantation of the $^{125}I$-labeled scaffolds in the backs of mice. Figure 7.5 illustrates the *in vivo* degradation profile of both HFIP-derived and aqueous-derived scaffolds. It was found that the radioactivity of both kinds of scaffolds was steadily and slowly decreased and eventually remained at around 45% of their initial radioactivity after 24 days. This result suggests that both kinds of scaffolds slowly degraded. In addition, the declining degradation patterns of the HFIP-derived and the aqueous-derived scaffolds were quite similar, indicating the similar degradability of those two

types of scaffolds. However, the radioactivity remaining in the aqueous-derived scaffolds started to be significantly lower than that of the HFIP-derived scaffold at the $24^{th}$ day ($p<0.05$), so the *in vivo* long-term degradation needed to be further investigated.

Recently, Wang et al. (2008) studied both the short-term and long-term degradation of HFIP-derived and aqueous-derived scaffolds by observing the residual scaffolds implanted subcutaneously in rats. They found that both the HFIP-derived and aqueous-derived scaffolds were well tolerated by the host animal, particularly the scaffolds prepared from the higher concentrated solution. However, the aqueous-derived scaffolds were completely degraded varying from six to beyond 12 months, while all of the HFIP-derived scaffolds persisted more than one year *in vivo*. Thus, the HFIP-derived and aqueous-derived scaffolds were slowly degradable materials, but the aqueous-derived scaffolds had a faster degradation by observation in the long-term study than the HFIP-derived scaffolds.

Figure 7.6 shows the release profile of bFGF from the HFIP-derived and aqueous-derived scaffolds in a comparison with the retention of the bFGF after injection. Apparently, by the injection of the bFGF solution, most of the bFGF disappeared after one day of the administration. In contrast, the release of bFGF from either HFIP-derived or aqueous-derived scaffolds was in a sustained fashion. However, the release profile from both kinds of scaffolds was similar because their short-term degradation behaviors *in vivo* were not different (see Figure 7.5). The prolongation of the *in vivo* release of the bFGF from both kinds of scaffolds can be observed for over two weeks. The primary cause of the release of bFGF from the scaffolds was the combination phenomena of the non-complexed bFGF diffusion (see Figure 7.3) and the release of bFGF by the scaffold's degradation. Beyond two weeks, about 25 to 31% of the bFGF was permanently entrapped in the scaffolds, and still remained even after almost one month from the implantation. This was attributable to the very slow degradation of the scaffolds as well as the strong interaction between the silk fibroin and the bFGF existing within the deeper part of the scaffold's wall.

To conclude, the *in vivo* studies indicate that the performance of both HFIP-derived and aqueous-derived scaffolds, in terms of the scaffold degradation and the release of bFGF, was similar because the study was not long enough to observe the differences in the scaffold degradation. However, it is expected that the bFGF will be further released from the scaffolds due to the scaffold's degradation.

## 7.5 Conclusion

The contributions from this present work are important for developing silk fibroin as a growth factor-releasing scaffold. The morphology of the three-dimensional porous silk fibroin scaffold prepared by different modes of processing displayed comparable pore size and structure. The slower degradation of the HFIP-derived scaffolds was attributable to a higher number of chain entanglements in the material as compared to the aqueous-derived scaffolds. The control of the chain entanglement might be the key to success in the future for improving the degradation of the silk fibroin material. The affinity between the silk fibroin and the bFGF is based on the electrostatic interaction. The primary factors that govern the release profile of the bFGF from the silk fibroin scaffolds used as the carrier matrix under *in vitro* enzymatic degradation conditions were the dispersion (along the depth of the scaffold's wall) of the bFGF existing in the carrier and the degradability of the scaffold. A longer period of the noticeable different *in vivo* degradation between the compared scaffolds may be due to the non-existence of the specific enzyme in the body as compared to the *in vitro* degradation. Although the bioactivity of bFGF upon *in vivo* release should be further evaluated, the sustainable release of bFGF over 2 weeks might enhance the *in vivo* efficacy of bFGF.

## 7.6 Acknowledgements

This work was supported by the Thailand Research Fund (through the Royal Golden Jubilee Ph.D. Program, i.e. RGJ grant) and The Petroleum and Petrochemical College, Chulalongkorn University. The authors wish to thank the Queen Sirikit Sericulture Center (Saraburi Province, Thailand) for supplying essential materials for this study.

## 7.7 References

Ayub, Z.H., Arai, M., Hirabayashi, K., 1993. Mechanism of the gelation of fibroin solution. Bioscience Biotechnology and Biochemistry, 57, 1910-1912.

Bolton AE, Hunter WM. (1973). The labeling of proteins to high specific radioactivities by conjugation to a $^{125}$I-containing acylating agent. Biochemical Journal, 133, 529–539.

Chang, G., Kim, H.-J., Kaplan, D.L., Vunjak-Novakovic, G., and Kandel, R.A. (2007). Porous silk scaffolds can be used for tissue engineering annulus fibrosus. European Spine Journal, 16, 1848-1857.

Chen WY, Rogers AA, Lydon MJ. (1992). Characterization of biologic properties of wound fluid collected during early stages of wound healing. The Journal of Investigative Dermatology, 99, 559–64.

Chen, C., Chuanbao, C., Xilan, M., Yin, T., and Hesun, Z. (2006). Preparation of non-woven mats from all-aqueous silk fibroin solution with electrospinning method. Polymer, 47, 6322-6327.

Chen, J., Minoura, N., Tanioka, A., (1994). Transport of pharmaceuticals through silk fibroin membrane. Polymer, 35, 2853-2856.

Cheng, Q., Peng, T.Z., Hu, X.B., Yang, F.Y., (2005). Charge-selective recognition at fibroin-modified electrodes for analytical application. Analytical and Bioanalytical Chemistry, 382, 80-84.

Freyman, T.M., Yannas, I.V., and Gibson, L.J. (2001) Cellular materials as porous scaffolds for tissue engineering. Progress in Materials Science, 46, 273-282.

Fujita, M., Ishihara, M., Morimoto, Y., Simizu, M., Saito, Y., Yura, H., Matsui, T., Takase, B., Hattori, H., Kanatani, Y., Kikuchi, M., and Maehara, T., (2005). Efficacy of Photocrosslinkable Chitosan Hydrogel Containing fibroblast growth factor-2 in a rabbit model of chronic myocardial infarction. Journal of Surgical Research, 126, 27–33.

Godspodarowicz, D., Cheng, J. (1986). Heparin protects basic and acidic FGF from inactivation. Journal of Cellular Physiology, 128, 475–484.

Greenwood, F.C., Hunter, M.W., and Glover, T.C. (1963). The preparation of $^{131}$I-labeled human growth hormone of high specific radioactivity. Biochemical Journal, 89, 114-123.

Hofmann, S., Hagenmuller, H., Koch, A.M., Muller, R., Vunjak-Novokovic, G., Rechenberg, B., Kaplan, D.L., Merkle, H.P., and Meinel, L. (2007). Control of in vitro tissue-engineered bone-like structures using human mesenchymal stem cells and porous silk scaffolds. Biomaterials, 28, 1152-1162.

Hokugo, A., Takamoto, T., Tabata, Y. (2006). Preparation of hybrid scaffold from fibrin and biodegradable polymer fiber. Biomaterials, 27, 61–67.

Huang, X., Yang, D., Yan, W., Shi, Z., Feng, J., Gao, Y., Weng, W., Yan, S. (2007). Osteochondral repair using the combination of fibroblast growth factor and amorphous calcium phosphate/poly(L-lactic acid) hybrid materials. Biomaterials, 28, 3091–3100.

Jeon, O., Ryu, S.H., Chung, J.H., Kim, B-S. (2005). Control of basic fibroblast growth factor release from fibrin gel with heparin and concentrations of fibrinogen and thrombin. Journal of Controlled Release, 105, 249–259.

Jin, H.-J., Park, J., Karageorgiou, V., Kim, U., Valluzzi, R., Cebe, P., and Kaplan, D.L. (2005). Water-stable silk films with reduced beta-Sheet content. Advanced Functional Materials, 15, 1241-1247.

Jiang, C., Wang, X., Gunawidjaja, R., Lin, Y-H., Gupta, M.K., Kaplan, D.L., Naik, R.R., Tsukruk, V.V. (2007). Mechanical Properties of Robust Ultrathin Silk Fibroin Films. Advanced Functional Materials, 17, 2229-2237.

Kanematsu, A., Marui, A., Yamamoto, S., Ozeki, M., Hirano, Y., Yamamoto, M., Ogawa, O., Komeda, M., and Tabata, Y. (2004). Type I collagen can function as a reservoir of basic fibroblast growth factor. Journal of Controlled Release, 99, 281-292.

Karageorgiou, V., Tomkins, M., Fajardo, R., Meinel, L., Snyder, B., Wade, K., Chen, J., Vunjak-Novokovic, G., and Kaplan, D.L. (2006). Porous silk fibroin 3-D scaffolds for delivery of bone morphogenetic protein-2 *in vitro* and *in vivo*. Journal of Biomedical Materials Research, 78A, 324-334.

Ki, C.S., Lee, K.H., Baek, D.H., Hattori, M., Um, I.C., Ihm, D.W., and Park, Y.H. (2007). Dissolution and wet spinning of silk fibroin using phosphoric acid/formic acid mixture solvent system. Journal of Applied Polymer Science, 105, 1605–1610.

Kim, H.J., Kim, H.S., Matsumoto, A., Chin, I.J., Jin, H.J., Kaplan, D.L. (2005a). Processing window for forming silk fibroin bimaterials into a 3D porous matrix. Australian Journal of Chemistry, 58, 716-720.

Kim, U-J., Park, J., Kim, H.J., Wada, M., and Kaplan, D.L. (2005b). Three-dimensional aqueous-derived biomaterial scaffolds from silk fibroin. Biomaterials, 26, 2775–
2785.

Kim. H.J., Kim, U-J., Leisk, G.G., Bayan, C., Georgakoudi, I., Kaplan, D.L. (2007). Bone regeneration on macroporous aqueous-derived silk 3-D scaffolds. Macromolecular Bioscience, 7, 643-655.

Kurane, A., Simionescu, D.T., and Vyavahare, N.R. (2007). In vivo cellular repopulation of tubular elastin scaffolds mediated by basic fibroblast growth factor. Biomaterials, 28, 2830-2838.

Lee, K.Y., and Yuk, S.H. (2007). Polymeric proteins delivery systems. Progress in Polymer Science, 32, 669-697.

Levenberg, S., and Langer, R. (2004). Advances in tissue engineering. Current Topic in Developmental Biology, 61, 113-134.

Li, C., Vepari, C., Jin, H-J., Kim, H.J., Kaplan, D.L. (2006). Electrospun silk-BMP-2 scaffoldsfor bone tissue engineering. Biomaterials, 27, 3115-3124.

Lind, M., Overgaard, S., Glerup, H., Soballe, K., Bunger, C. (2001). Transforming growth factor-b1 adsorbed to tricalciumphosphate coated implants increases peri-implant bone remodeling. Biomaterials, 22, 189-193.

Liu, H., Ge, Z., Wang, Y., Toh, S.L., Sutthikhum, X., and Goh, J.C.H. (2007). Modification of sericin-free silk fibers for ligament tissue engineering application. Journal of Biomedical Materials Research Part B-Applied Biomaterials, 82B: 129-138.

Liu, H., Fan, H., Wang, Y., Toh, S.L., and Goh, J.C.H. (2008). The interaction between a combined knitted silk scaffold and microporous silk scaffold with human meschymal stem cells for ligament tissue engineering. Biomaterials, 29, 662-674.

Marolt, D., Augst, A., Freed, L.E., Vepari, C., Fajardo, R., Patel, N., Gray, M., Farley, M., Kaplan, D.L., and Vunjak-Novokovic, G. (2006). Bone and cartilage tissue constructs grown using human bone marrow stromal cells, silk scaffolds and rotating bioreactors. Biomaterials, 27, 6138-6149.

Mauney, J., Nguyen, T., Gillen, K., Kirker-Head, C., Gimble, J.M., and Kaplan, D.L. (2007). Engineering sdipose-like tissue in vitro and in vivo utilizing human bone marrow and adipose-derived mesenchymal stem cells with silk fibroin 3D scaffolds. Biomaterials, 28, 5280-5290.

Meinel, L., Hofmann, S., Karageorgiou, V., Zichner, L., Langer, R., Kaplan, D.L., and Vunjak-Novakovic, G. (2004a) Engineering cartilage-like tissue using human mesenchymal stem cells and silk protein scaffolds. Biotechnology and Bioengineering, 88, 379-391.

Meinel, L., Karageorgiou, V., Hofmann, S., Fajardo, R., Snyder, B., Li, C.M., Zichner, L., Langer, R., Vunjak-Novakovic, G., and Kaplan, D.L. (2004b) Engineering bone-like tissue in vitro using human bone marrow stem cells and silk scaffolds. Journal of Biomedical Material Research: Part A, 71A, 25-34.

Meinel, L., Hofmann, S., Karageorgiou, V., Kirker-Head, C., McCool, J., Gronoxicz, G., Zichner, L., Langer, R., Vunjak-Novakovic, G., and Kaplan, D.L. (2005). The inflammatory responses to silk films in vitro and in vivo. Biomaterials, 26, 147-155.

Meinel, L., Betz, O., Fajardo, R., Hofmann, S., Nazarian, A., Cory, E., Hilbe, M., McCool, J., Langer, R., Vunjak-Novokovic, G., Merkle, H.P., Rechenberg, B., Kaplan, D.L., and Kirker-Head, C. (2006). Silk based biomaterials to heal critical sized femur defects. Bone, 39, 922-931.

Mizuno, K., Inoue, H., Hagiya, M., Shimizu, S., Nose, T., Shimohigashi, Y., Nakamura, T. (1994). Hairpin loop and second kringle domain are essential sites for heparin binding and biological activity of hepatocyte growth factor, Journal of Biological Chemistry, 269, 1131–1136.

Nazarov, R., Jin, H.J., and Kaplan, D.L. (2004). Porous 3-D scaffolds from regenerated silk fibroin. Biomacromolecules, 5, 718–726.

Nicole SG, Isik F, Heimbach DM, Gordon D. (1994). Basic fibroblast growth factor in the early human burn wound. Journal of Surgical Research, 56, 226–34.

Ono I, Gunji H, Zhang JZ, Maruyama K, Kaneko F. (1995). A study of cytokines in burn blister fluid related to wound healing. Burns, 21, 352–5.

Pike, D.B., Cai, S., Pomraning, K.R., Firpo, M.A., Fisher, R.J., Shu, X.Z., Prestwich, G.D., Peattie, R.A. (2006). Heparin-regulated release of growth factors in vitro and angiogenic response in vivo to implanted hyaluronan hydrogels containing VEGF and bFGF. Biomaterials, 27, 5242–5251.

Radomsky ML, Thompson AY, Poser JW. (1998). Potential role of fibroblast growth factor in enhancement of fracture healing. Clinical Orthopaedics and Related Research, 355S, 283–93.

Roghani, M., Mansukhani, A., Dell'Era, P., Bellosta, P., Basilico, C., Rifkin, D., Moscatelli, D. (1994). Heparin increases the affinity of basic fibroblast growth factor for its receptor but is not required for binding. Journal of Biological Chemistry, 269, 3976–3984.

Ryu, W.H., Huang Z., Prinz, F.B., Goodman, S.B., Fasching, R. Biodegradable micro-osmotic pump for long-term and controlled release of basic fibroblast growth factor. Journal of Controlled Release, 124, 98-105.

Sakiyama-Elbert, S.E., Hubbell, J.A. (2000). Development of fibrin derivatives for controlled release of heparin-binding growth factors. Journal of Controlled Release, 65, 389–402.

Shen, H., Hu, X., Bei, J., Wang, S. (2008). The immobilization of basic fibroblast growth factor on plasma-treated poly(lactide-co-glycolide). Biomaterials, 29, 2388-2399

Shenoy, S.L., Bates, W.D., Frisch, H.L., Wnek, G.E. (2005). Role of chain entanglements on fiber formation during electrospinning of polymer solutions: good solvent, non-specific polymer polymer interaction limit. Polymer, 46, 3372-3384.

Sukigara, S., Gandhi, M., Ayutsede, J., Micklus, M., and Ko, F. (2003). Regeneration of *Bombyx mori* silk by electrospinning—part 1: processing parameters and geometric properties. Polymer, 44, 5721–5727.

Tabata, Y., Hijikata, S., and Ikada, Y. (1994). Enhanced vascularization and tissue granulation by basic fibroblast growth factor impregnated in gelatin hydrogels. Journal of Controlled Release, 31, 189-199.

Tabata, Y., and Ikada, Y. (1999a) Vascularization effect of basic fibroblast growth factor released from gelatin hydrogels with different biodegradabilities, Biomaterials, 20, 2169-2175.

Tabata Y, Nagano A, Ikada Y. (1999b). Biodegradation of hydrogel carrier incorporating fibroblast growth factor. Tissue Engineering, 5, 127–138.

Tabata, Y., Nagano, A., Muniruzzaman, Md., Ikada, Y. (1998). In vitro sorption and desorption of basic fibroblast growth factor from biodegradable hydrogels, Biomaterials, 19, 1781-1789.

Tabata, Y. (2005a). Significant role of cell scaffolding and DDS technology in tissue regeneration: tissue engineering strategies. International Congress Series, 1284, 257-265.

Tabata, Y. (2005b). Significance of release technology in tissue engineering. Drug Delivery Today, 10, 1639-1646.

Tao, J., and Shivekumar, S. (2007). Molecular weight dependent structural regimes during the electrospinning of PVA. Materials Letters, 61, 2325-2328.

Tessler, S., Rockwell, P., Hicklin, D., Cohen, T., Levi, B.Z., Witte, L., Lemischka, I.R., Neufeld, G., (1994). Heparin modulates the interaction of VEGF165 with soluble and cell associated flk-1 receptors, Journal of Biological Chemistry, 269, 12456– 12461.

Uebersax, L., Mattotti. M., Papaloizos, M., Merkle, H.P., Gander, B., and Meinel, L. (2007) Silk fibroin matrices for the controlled release of nerve growth factor (NGF). Biomaterials 28, 4449-4460.

Uebersax, L., Merkle, H.P., and Meinel, L. (2008). Insulin-like growth factor I releasing silk fibroin scaffolds induce chondrogenic differentiation of human mesenchymal stem cells. Journal of Controlled Release, 127, 12-21.

Um, I.C., Kweon, H.Y., Lee, K.G., Park, Y.H. (2003). The role of formic acid in solution stability and crystallization of silk protein polymer. International Journal of Biological Macromolecules, 33, 203–213.

Um, I.C., Kweon, H.Y., Lee, K.G., Ihm, D.W., Lee, J.-H., Park, Y.H. (2004). Wet spinning of silk polymer I. Effect of coagulation conditions on the morphological feature of filament. International Journal of Biological Macromolecules, 34, 89–105.

Wang, Y., Kim, U-J., Blasioli, D.J., Kim, H-J., Kaplan, D.L. (2005). In vitro cartilage tissue engineering with 3D porous aqueous-derived silk scaffolds and mesenchymal stem cells. Biomaterials, 26, 7082-7094.

Wang, Y., Blasioli, D.J., Kim, H-J., Kim, H.S., Kaplan, D.L. (2006). Cartilage tissue engineering with silk scaffolds and human articular chondrocytes. Biomaterials, 27, 4434-4442.

Wang, X., Wenk, E., Hu, X., Castro, G.R., Meinel, L., Wang, X., Li, C., Merkle, H., Kaplan, D.L. (2007a). Silk coatings on PLGA and alginate microspheres for protein delivery. Biomaterials, 28, 4161–4169.

Wang, X., Wenk, E., Matsumoto, A., Meinel, L., Li, C., Kaplan, D.L. (2007b). Silk microspheres for encapsulation and controlled release, Journal of Controlled Release, 117, 360–370.

Wang, X., Kluge, J.A., Leisk, G.G., Kaplan, D.L. (2008). Sonication-induced gelation of silk fibroin for cell encapsulation. Biomaterials, 29, 1054-1064.

Wang, Y., Rudym, D.D., Walsh, A., Abrahamsen, L., Kim, H-J., Kim, H.S., Kirker-Head, C., Kaplan, D.L. (2008). In vivo degradation of three-dimensional silk fibroin scaffolds. Biomaterials, In press.

Wissink, M.J.B., Beernink, R., Poot, A.A., Engbers, G.H.M., Beugeling, T., van Aken, W.G., Feijen, J. (2000). Improved endothelialization of vascular grafts by local release of growth factor from heparinized collagen matrices. Journal of Controlled Release, 64,103–114.

Wongpanit, P., Sanchavanakit, N., Pavasant, P., Bunaprasert, T., Tabata, Y., Rujiravanit, R. (2007a) Preparation and characterization of chitin whisker-reinforced silk fibroin nanocomposite scaffolds. European Polymer Journal, 43, 4123–4135.

Wongpanit, P., Tabata, Y., and Rujiravanit, R. (2007b). Miscibility and biodegradability of silk fibroin/carboxymethyl chitin blend films. Macromolecular Bioscience, 7, 1258-1271.

Yeo, J-H., Lee, K-G., Lee, Y-W. and Kim, S.Y. (2003). Simple preparation and characteristics of silk fibroin microsphere. European Polymer Journal, 39, 1195-1199.

Zarkoob, S., Eby, R.K., Reneker, D.H., Hudson, S.D., Ertley, D. and Adams, W.W. (2004). Structure and morphology of electrospun silk nanofibers. Polymer, 45, 3973–3977.

Zarkoob, S., Reneker, D.H., Eby, R.K., Hudson, S.D., Ertley, D. and Adams, W.W. (1998). Structure and morphology of nanoelectrospun silk fibers. Polymer Preprints, 39, 244-245.

Zhang, Y.-Q., Shen, W.-D., Xiang, R.-L., Zhuge, L.-J., Gao, W.-J. and Wang, W.-B. (2007). Formation of silk fibroin nanoparticles in water-miscible organic solvent and their characterization. Journal of Nanoparticle Research, 9, 885–900.

Zhou, C.Z., Confalonier, F., Medina, N., Zivanovic, Y., Esnaullt, C., Yang, L., Jacquet, M., Jänin, J., Duguet, M., Perasso, R., Li, Z.G., (2000). Fine organization of *Bombyx Mori* fibroin heavy chain gene. Nucleic Acids Research, 28, 2413-2419.

**Table 7.1** Isoelectric points of the fibroin proteins determined from various methodologies

| Isoelectric point | Method of determination | Method of Regeneration | | Reference |
|---|---|---|---|---|
| | | Degumming | Dissolving | |
| 3.9 | Electrophoretic mobility | 0.05% $Na_2CO_3$ | $CaCl_2$/Ethanol/Water | Malay et al., 2007 |
| 4.22 | Calculation | -[b] | -[b] | Zhou et al., 2000 |
| 3.8-3.9 | -[a] | 0.5% $Na_2CO_3$ | $CaCl_2$/Ethanol/Water | Ayub et al., 1993 |
| 4.5 | Membrane potential | 0.5% $Na_2CO_3$ | $CaCl_2$/Ethanol/Water | Chen et al., 1994 |
| 4.5 | Membrane potential | 0.5% $Na_2CO_3$ | $CaCl_2$/Ethanol/Water | Cheng et al., 2005 |

[a] = The authors raised without any comment.

[b] = The raw sequence data were obtained by the Fragment Assembly program in Seqlab of the Genetics Computer Group sequence analysis software package version 10.0.

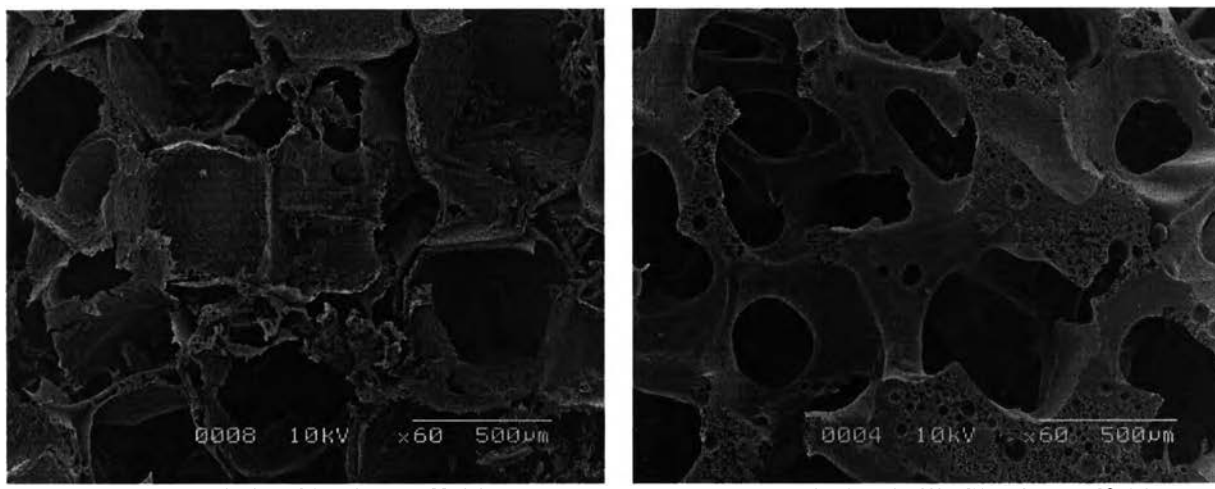


(A) HFIP-derived silk fibroin scaffold (B) Aqueous-derived silk fibroin scaffold

Figure 7.1 Cross-sectional morphology of (A) the HFIP-derived and (B) the aqueous-derived silk fibroin scaffold. The average pore size of the HFIP-derived and aqueous-derived scaffolds was 479±130 and 473±146 μm, respectively.

(A)

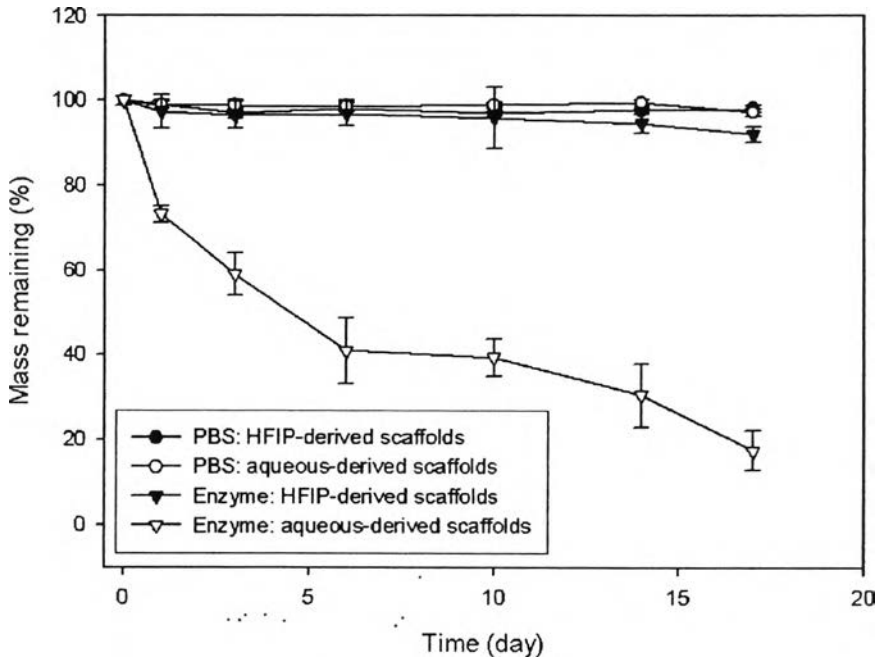


(B)

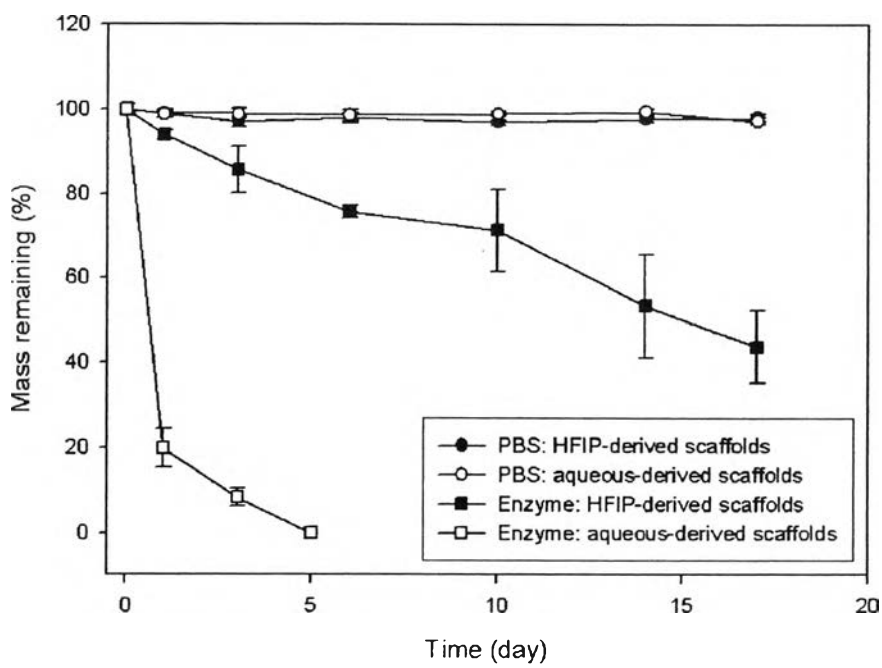


Figure 7.2 *In vitro* degradation of HFIP-derived and aqueous-derived silk fibroin scaffolds. The concentration of protease XIV in the PBS was (A) 0.05 and (B) 0.5 $mg \cdot ml^{-1}$.

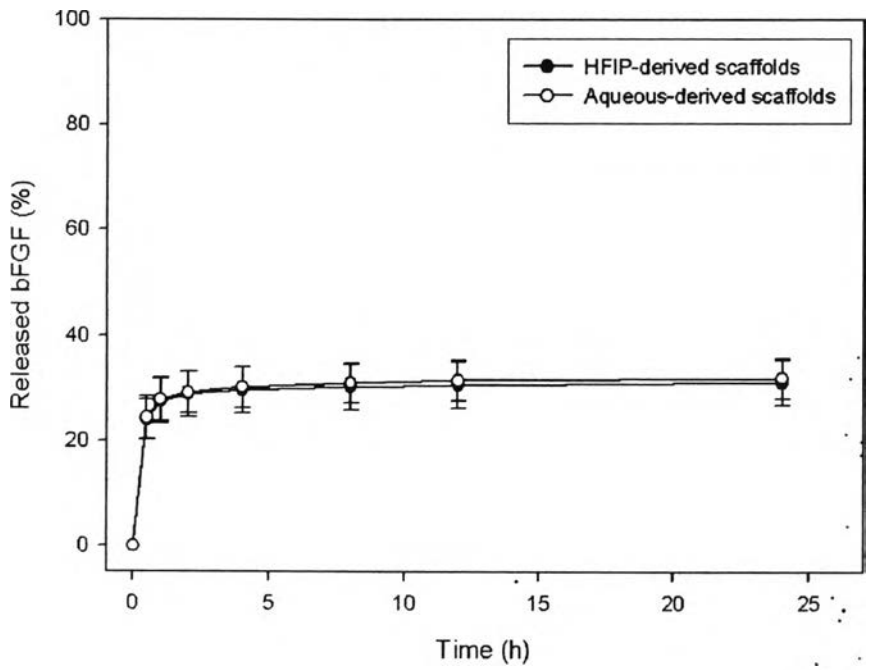


Figure 7.3 Release profile of the bFGF from bFGF-impregnated HFIP-derived or aqueous-derived silk fibroin scaffolds submerged in PBS under strong shaking with periodic replacement with fresh PBS.

(A)

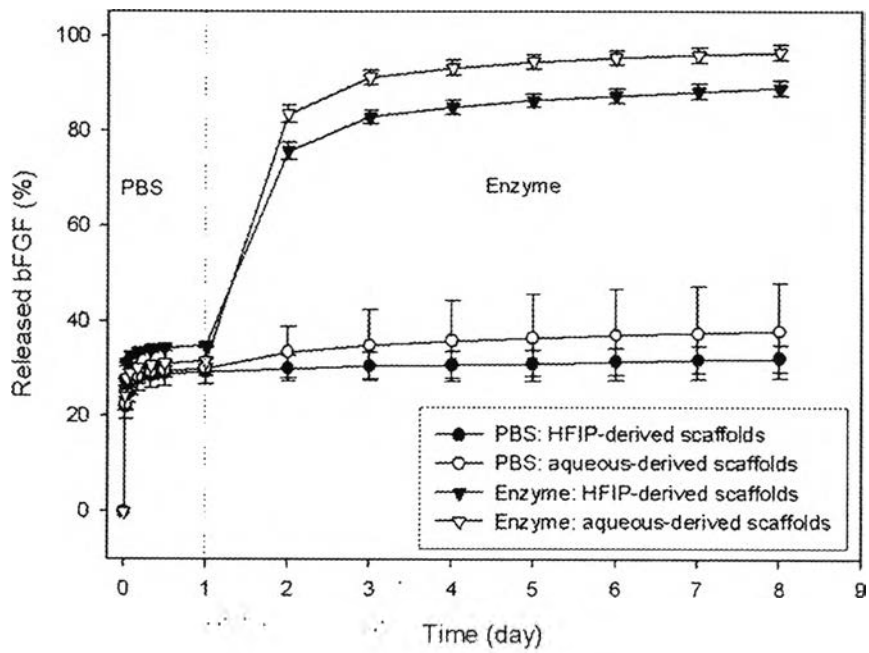


(B)

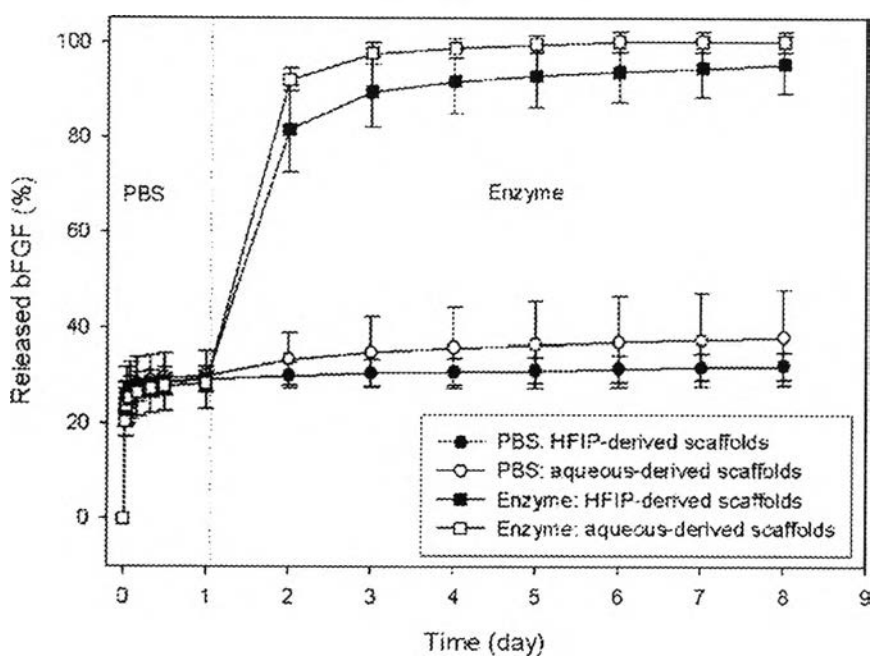


Figure 7.4 Release profile of the bFGF from bFGF-impregnated HFIP-derived or aqueous-derived silk fibroin scaffolds under the enzymatic degradation of the silk fibroin. After 24 h releasing in PBS, the release media was replaced by PBS containing protease XIV at (A) 0.05 or (B) 0.5 $mg \cdot ml^{-1}$.

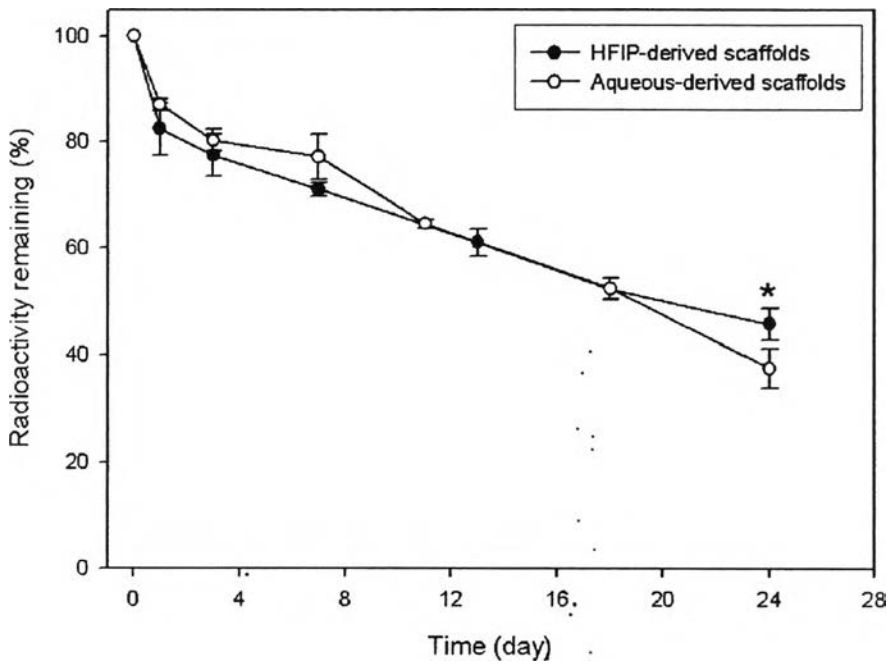


Figure 7.5 *In vivo* degradation of HFIP-derived or aqueous-derived silk fibroin scaffolds. Patterns of declining radioactivity in the backs of mice after subcutaneous implantation of the $^{125}$I-labeled silk fibroin scaffolds. *, $P< 0.05$; significant against the group of aqueous-derived scaffolds.

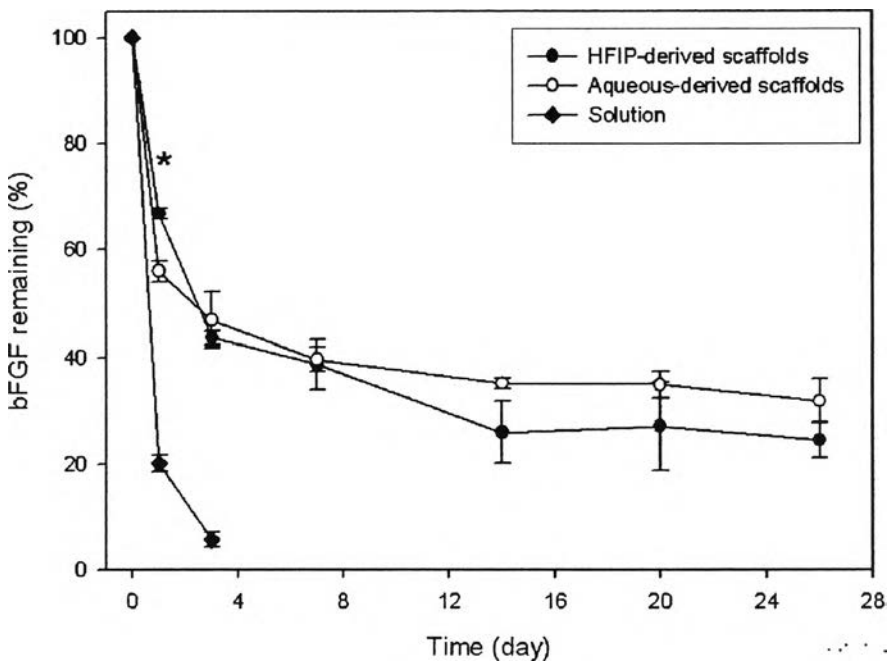


Figure 7.6 *In vivo* release of the bFGF from bFGF-impregnated scaffolds. Patterns of declining radioactivity in the backs of mice after subcutaneous implantation of $^{125}$I-labeled bFGF (●) impregnated in HFIP-derived or (○) aqueous-derived silk fibroin scaffolds, and the declining radioactivity of the $^{125}$I-labeled bFGF (♦) by subcutaneous injection. *, $P< 0.05$; significant compared to every other groups.